Orientation of a Chiral Filament in a Viscous Four-Roll Flow Field

Youn J. Kim*
(Received January 27, 1996)

Using singularity method, the general Stokes flow characteristics present for a chiral filament in the rectangular hyperbolic flow were studied. To find the force and torque required to move a chiral filament in any direction, Johnson's slender body theory was applied. These results were then expressed in the context of the resistance coefficients, so that all motions can be described at once for a given orientation. The present LU-decomposition method can be used for advantage. For long trajectories, the direct solver runs in approximately a tenth of the time of the successive iteration scheme. Trajectories of a chiral filament in a given flow field are prepared for various values of the buoyancy parameter Y. The results of this analysis may be used to predict the behavior of suspensions and to develop experimental apparatus.

Key Words: Low Reynolds Number, Slender Body Theory, Singularity Method, Euler Angles, Trajectories

1. Introduction

The creeping motion of particles in a viscous, incompressible fluid occurs in many physical processes and in engineering problems that have no significant inertial effects. The literature has shown the results of the particle orientation in different kinds of flows by using both analytical, numerical and experimental techniques, such as, the problems of the motion of red blood cells in the microcirculation (Goldsmith 1971), sedimentology, molecular orientation, anisotropy of various physical properties, short fiber-reinforced material processing and rheological behavior of solutions (Stover and Cohen 1990, Kim and Karrila 1991). Another example of slender body motion in Stokes flows is racemic mixtures, which are suspensions of stereoisomers, namely the *cis*- and *trans*-isomer, identical in chemical formula and bond type, but different in shape. With the metal ion lying in the center, the two chloride ligands in the chemical formula $Pt(NH_3)_2Cl_2$ can either lie opposite to one another or on the same side of the molecule. The *cis*-isomer is a powerful anticancer drug. The *trans*-isomer is not (Boikess and Edelson 1981). A similar problem occurs with helical shaped molecules, which can have either 'left' and 'right' screw senses. In the case of L-dopamine, for example, only one screw sense works in the body. Since separation of these particles is impossible by centrifugation or diffusion, the motion of slender helical particles is of interest under different Stokes flow conditions.

To solve these motions of chiral filaments in Stokes flow, we may use Johnson's integral equation (see Johnson 1977, 1980) involving a distribution of stokeslets, or point force singularities, along the filament centerline interest. If such a filament is of length 2ℓ and has a cross-sectional diameter of d, an expansion of the velocity field about such a filament is made in terms of the slenderness parameter $\varepsilon = d/2\ell$. From this information, we can find directly the independent force and torque coefficients needed to solve for these motions.

The motion of a single rigid ellipsoid of revolution in a constant shear flow at low Reynolds

* School of Mechanical Engineering, Institute of Advanced Machinery and Technology, Sung Kyun Kwan University, 300 Chunchun-dong, Jangan-gu, Suwon, 440-746 KOREA

number was found in analytic form by Jeffery (1922) and was verified experimentally by many researchers (Goldsmith and Mason 1971, Chaffey, Takano and Mason 1965). Jeffery's oft-quoted solution has since provided the starting point for a multitude of theoretical investigations relating to the various flow circumstances. However, the particle with simple form such as ellipsoid or sphere is less encountered in practice. Therefore, the purpose of this paper is to provide a better understanding of the low Reynolds number motion of three-dimensional particles in two-dimensional, rectangular hyperbolic shear flow, the so called four-roll flow field.

In addition, it should be stressed that the solutions pursued here are limited to rigid particles, with no consideration of Brownian motion or forces of electrical origin, and to particles with uniform density, so that there are no gravitational torques arising from a displacement of the center of mass from the center of buoyancy.

2. Formulation of Problems

2.1 Mathematical formulation

Consider a viscous, incompressible fluid, sheared at a rate characterized by the velocity gradient $\nabla\vec{u}$, and uniform throughout the fluid. In this field, the motion of a chiral filament with surface S_f and the ensuing velocity $\vec{V}$ and pressure p can be assumed that satisfies the following quasi -static Stokes equations:

$$\nabla^2 \vec{V} = \frac{1}{\mu}\nabla p, \quad \nabla \cdot \vec{V} = 0 \tag{1}$$

in which μ is the fluid viscosity.

Figure 1 shows a sketch of a chiral filament and the orientation of the reference systems useful in describing the filament. A helical system can be established in reference to the space-fixed coordinate system and the local vectors originated on the generic curve of the helix. The centerline of a screw-sensed particle is described by

$$\begin{aligned} \vec{r} &= x\hat{\boldsymbol{i}} + y\hat{\boldsymbol{j}} + z\hat{\boldsymbol{k}} \\ &= a\cos\frac{s}{c}\hat{\boldsymbol{i}} + ha\sin\frac{s}{c}\hat{\boldsymbol{j}} + b\frac{s}{c}\hat{\boldsymbol{k}} \end{aligned} \tag{2}$$

where s represents the arc length along the fila-

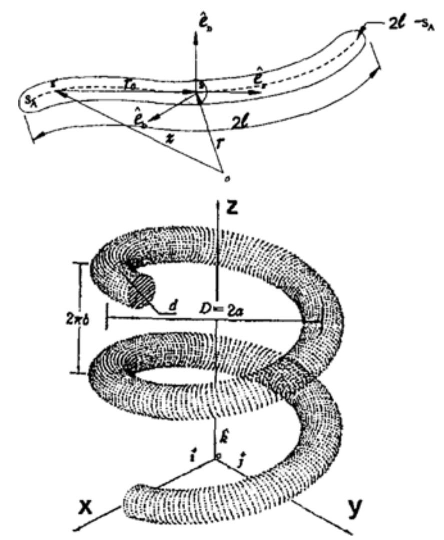

Fig. 1 A right-handed chiral filament and coordinates

ment centerline; a and b are constant parameters; c is $\sqrt{a^2+b^2}$; and $\hat{\boldsymbol{i}}$, $\hat{\boldsymbol{j}}$, and $\hat{\boldsymbol{k}}$ are unit vectors in cartesian directions. Here h is equal to plus or minus one for a right- or left-handed chiral filament, respectively. Eq. (2), also, shows that the central helix has a pitch $2\pi b$, pitch angle $\beta = \tan^{-1}(b/a)$, and is coiled along a cylinder with diameter $D(=2a)$. The overall length of a coil consisting of n turns (where n need not be an integer) is $L=2\pi nb$.

The non-slip boundary condition on the filament surface is:

$$\vec{V} = \vec{U}_o + \vec{\omega} \times \vec{r}_o \text{ on } S_f \tag{3}$$

where $\vec{U}_o$ and $\vec{\omega}$ denote the velocity on the surface of the chiral filament translating and rotating through the fluid medium, respectively, and $\vec{r}$ the position vector of a point relative to an origin at o in a three-dimensional Euclidean space (see Fig. 1).

At large distances from the filament surface the original uniform shear field $\vec{u}$ is not disturbed, therefore,

$$\vec{V} \rightarrow \vec{u} = \vec{u}_o + \vec{r}_o \cdot \nabla\vec{u} \text{ as } |\vec{r}| \rightarrow \infty \tag{4}$$

in which $\vec{u}_o$ is the approach velocity of the undisturbed flow at o Also, the trace of $\vec{u}$ should be zero to satisfy the conservation of mass for incompressible flow.

Using Serret-Frenet formulas (see Struik 1950), the unit vectors in the tangential, binormal, and normal directions are defined as

$$\hat{e}_s=\frac{\partial \vec{r}}{\partial s}$$
$$\hat{e}_b=\frac{1}{k}\frac{\partial \hat{e}_s}{\partial s}$$
$$\hat{e}_n=\hat{e}_s\times\hat{e}_b \tag{5}$$

where $k(=k'a)$ is the local non-dimensional curvature of the filament centerline, which is defined as

$$k'=\frac{a}{a^2+b^2}=\frac{a}{c^2}=\frac{\cos^2\beta}{a} \tag{6}$$

These three unit vectors ($\hat{e}_n$, $\hat{e}_s$, $\hat{e}_b$) form the mutually orthogonal unit vectors. This orthogonality of a coordinate system can be achieved by simply rotating the basis formed by the Frenet frame $\hat{e}_b$ and $\hat{e}_n$ around the filament curve length. Also, the Serret-Frenet formulas give

$$\frac{\partial \hat{e}_n}{\partial s}=\tau'\ \hat{e}_b-k'\hat{e}_s$$
$$\frac{\partial \hat{e}_b}{\partial s}=\tau'\ \hat{e}_n \tag{7}$$

where τ' is the torsion of the helix (its dimensionless form denoted as $\tau=\tau'a$), defined as

$$\tau'=\frac{b}{a^2+b^2}=k'\tan\beta=\frac{\sin\beta\cos\beta}{a} \tag{8}$$

Using Eqs. (2) and (5), one finds the unit vectors for helicoidal coordinates to be

$$\hat{e}_n=h\frac{b}{c}\sin u\hat{\boldsymbol{i}}-\frac{b}{c}\cos u\hat{\boldsymbol{j}}+h\frac{a}{c}\hat{\boldsymbol{k}}$$
$$\hat{e}_s=-\frac{a}{c}\sin u\hat{\boldsymbol{i}}+h\frac{a}{c}\cos u\hat{\boldsymbol{j}}+\frac{b}{c}\hat{\boldsymbol{k}} \tag{9}$$
$$\hat{e}_b=-\cos u\hat{\boldsymbol{i}}-h\sin u\hat{\boldsymbol{j}}$$

In addition, the relavent curvature and torsion of filament whose centerline does not reapproach itself can be written as:

$$\frac{1}{k}=1+\left(\frac{L/D}{n\pi}\right)^2,\quad \tau=\frac{L/D}{n\pi}k \tag{10}$$

2.2 Slender body theory

As stated in Johnson (1980), the boundary condition at the filament surface becomes an integral of the singularities along the filament centerline. With the slenderness limit the extensive singular solutions could be expressed by a simple form as the only surviving singularity, i.e., stokeslet strength $\boldsymbol{\alpha}$. The results display the leading contribution coming from the vicinity of the point where the velocity boundary condition is being applied, plus a regular integral over the length of the filament centerline. Therefore, the velocity distribution along the surface of the filament may be written as:

$$V_\nu(s)=\boldsymbol{\alpha}_\nu(s)L_\nu+\int_{s_A}^{2\ell-s_A}K_\nu(r_o\,;\,\boldsymbol{\alpha})\,ds'$$
$$(\nu=\text{n, s, b}) \tag{11}$$
$$K_\nu(\boldsymbol{r}_o\,;\,\boldsymbol{\alpha})=\frac{\boldsymbol{\alpha}_\nu(s')}{r_o}+\frac{[\boldsymbol{\alpha}(s')\cdot\boldsymbol{r}_o]r_{o\nu}}{r_o^3}-\frac{D_\nu\boldsymbol{\alpha}_\nu(s)}{|s-s'|} \tag{12}$$

where $L_s=2(2L-1)$, $L_n=L_b=2L+1$, $L=\ln(2/\varepsilon)$ and $D_n=D_b=1$, $D_s=2$.

The linearity of the above Stokes equations and boundary conditions allows complex flows to be solved by adding the effects of several terms which describe the flow in which the particle immersed. Furthermore, the extent of the distribution of the stokeslets is guided by the exact solution for a prolate spheroid and is taken to lie between the generalized foci of the particle, i.e., the singularity is nonzero only for $s_A\le S_f\le 2\ell-s_A$ where $s_A=\ell[1-\sqrt{1-\varepsilon^2}]$ is the generalized eccentricity in the slender body limit $\varepsilon\ll 1$.

The vector components in the above integrand K_ν refer to the unit vectors $\hat{e}_n$, $\hat{e}_s$, and $\hat{e}_b$ at a field point s where the boundary condition is to be satisfied. However, the terms in the integrand will blow up when the field point and the source point coincide. This is due to the fact that every field point is really at the field/filament interface surrounding the particle, while every source point s' is at the centerline of the filament. In order to avoid these difficulties for integration and to get proper form of the kernel at $s=s'$, Taylor series expansion on r_o was performed, and the magnitude of the vector $\vec{r}_o$ can be rewritten as:

$$|r_o|=|s-s'|\sqrt{1-\frac{a^2}{12c^4}(s-s')^2+\cdots} \tag{13}$$

Also, we can derive the special forms of the integrand for the case in which the source and field points are the same, namely,

$$K_n = 0$$
$$K_s = -\frac{a}{2c^2}\alpha_b(s) \qquad (14)$$
$$K_b = -\frac{a}{2c^2}\alpha_s(s)$$

2.3 Four-roll flowfield

Leal (1984) showed that the configuration of nature of flow as a continuous, one parameter family of the form, if the flows are idealized as linear, and two-dimensional, as follows:

$$\vec{u} = G^*\Gamma \cdot \vec{s} \qquad (15)$$

with $\Gamma \equiv \begin{bmatrix} 1+\lambda & 1-\lambda & 0 \\ -(1-\lambda) & -(1+\lambda) & 0 \\ 0 & 0 & 0 \end{bmatrix}$

where G^* is the magnitude of the velocity gradient. In this analysis, we choose the case $\lambda=1$ which corresponds to the kinematics of the hyperbolic, pure-straining flow. Figure 2 shows the schematic representation of two-dimensional hyperbolic flow which is typically produced by four-roll mill. Here the streamlines are given by $s_1 s_2 = \text{constant}$. The velocity field, therefore, considered here with ($G \equiv 4G^*$) is

$$u = \frac{1}{2}G\ s_1, \quad v = -\frac{1}{2}G\ s_2, \quad w = 0 \qquad (16)$$

and then we may have the rate of strain dyadic of the undisturbed flow, using unit vectors (here the

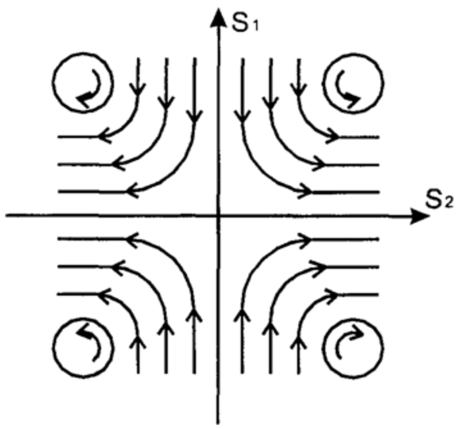

Fig. 2 A schematic diagram of the hyperbolic extensional flow

unit vectors in space-fixed coordinate are denoted by $\hat{s}_1$, $\hat{s}_2$ and $\hat{s}_3$) as

$$S = \frac{1}{2}(\nabla\vec{u} + \nabla\vec{u}^{\dagger})$$
$$= \frac{1}{2}(\hat{s}_1\hat{s}_1 - \hat{s}_2\hat{s}_2) \qquad (17)$$

in which the superscript $(\ )^{\dagger}$ denotes the transpose of tensor. However, the angular velocity of a fluid particle, which is defined as

$$\vec{\omega}_f = \frac{1}{2}\nabla \times \vec{u} \qquad (18)$$

may be written for this case as zero value, since the considered flow is irrotational.

2.4 Hydrodynamic resistance tensors

Brenner (1964) has shown that the force and torque at the center of mass of the filament are proportional to the first powers of the translational and angular velocities and of the shear rate of strain, the constants of proportionality being a set of second- and third-rank tensors. These can be written as the following dimensionless formulas:

$$F = -[K \cdot (U_c - u_c) + C_c^{\dagger} \cdot (\omega_c - \omega_f) + \Phi_c : S] \qquad (19)$$
$$T_c = -[C_c \cdot (U_c - u_c) + \Omega_c \cdot (\omega_c - \omega_f) + \Psi_c : S] \qquad (20)$$

Here the double dot products of polyadics are defined as

$$A : S = \Sigma A_{ijk}\hat{i}\hat{j}\hat{k} : S_{mn}\hat{m}\hat{n}$$
$$= \Sigma A_{ijk}S_{mn}\hat{i}(\hat{k}\cdot\hat{m})(\hat{j}\cdot\hat{n})$$
$$= \delta_{km} \quad = \delta_{jn} \qquad (21)$$

where δ_{km}, δ_{jn} represent the Kronecker delta, and $\hat{m}$, $\hat{n}$ are arbitrary unit vectors.

The K, C_c, and Ω_c are second-rank tensors which are called the translation, coupling, and rotation tensors, respectively. The third-rank tensors Φ_c and Ψ_c, which are called by Brenner (1964) the shear-force and shear-torque triadics, are symmetric in their second and third subscripts, and three elements in each tensor can be set to zero in keeping with the incompressibility condition. These hydrodynamic resistance coefficients depend on the particle shape, and not on the nature of the flow. With the aid of a characteristic filament dimension ℓ, the translational tensor K has the dimension ℓ. The dimensions of C_c and Φ_c are ℓ^2, and those of Ω_c and Ψ_c are ℓ^3, respectively.

In order to determine these tensors, the motion of a chiral filament in a rectangular hyperbolic flow can be divided into three cases of sub-problems, those of the pure shear field, the translational and rotational field, and the uniform shear field (see Brenner 1964). The first two problems are variants of the prototype problem, namely, that a finding the force and torque due to a given distribution of velocity at the particle surface in an unbounded fluid at rest at infinity. The solution of the second sub-problem leads to the second-rank tensors. The third one does not contribute to the force and torque on the particle.

Kim and Rae (1991) have shown a comparison of the numerical values of the hydrodynamic resistance coefficients for a slender needle whose equatcrial diameter is one-hundredth of its length calculated by the slender body theory and by the analytical formulas (Happel and Brenner 1986). This theory incorrectly predicted the resistance coefficients to rotation about the centerline of a straight fiber to be zero, since all of the rotational resistance computed from the slender body theory comes from the fact that the particle has some curvature somewhere. However, the comparisons between their results and the analytic formulas have shown excellent agreement (see Kim and Rae 1991).

With the knowledge of these 51 scalar coefficients, i.e., each six for the translation and rotation tensors, nine for the coupling tensor, and each fifteen elements of the shear-force and shear-torque triadics, the hydrodynamic force and torque on a chiral filament undergoing given translational and rotational motions in a rectangular hyperbolic flow are completely defined.

3. Methods of Solution

In order to compute the singularity distribution on the filament centerline, more efficient algorithm was developed. Since the successive iteration method, originally used by Johnson, took a great deal of CPU time to run due to use of too many panels in the iteration scheme of Johnson's equation, the LU-decomposition scheme, which was taken from Press, et al. (1986), was applied.

From the discrete integration of the singularity distribution, Eq. (11), we have obtained a set of linearly independent equations of the form, as follows:

$$\{V\}=[M_{km}]\{\alpha\} \tag{22}$$

Each element of M_{km} is a 3×3 submatrix that is a function only of the filament geometry.

Off-diagonal submatrices, evaluated directly from Johnson's integral equation, appear as follows:

$$[M_{km}]_{k\neq m}=\Delta s\ \xi(s'_m)\begin{bmatrix} \frac{1}{r_o}+\frac{r_{on}^2}{r_o^3} & \frac{r_{on}r_{os}}{r_o^3} & \frac{r_{on}r_{ob}}{r_o^3} \\ \frac{r_{os}r_{on}}{r_o^3} & \frac{1}{r_o}+\frac{r_{os}^2}{r_o^3} & \frac{r_{os}r_{ob}}{r_o^3} \\ \frac{r_{ob}r_{on}}{r_o^3} & \frac{r_{ob}r_{os}}{r_o^3} & \frac{1}{r_o}+\frac{r_{ob}^2}{r_o^3} \end{bmatrix} \tag{23}$$

where $\xi(s)$ is the weighting function, $r_{o\nu}$ is the distance vector from source point to field point in the field point coordinates, both points being on the body, and r_o is the scalar distance between the two points.

The diagonal submatrices produced by Eq. (11), which use the special case for the kernel (Eq. 12) for $s=s'$ given in Eq. (14), are shown here:

$$[M_{kk}]=\begin{bmatrix} L_n & 0 & 0 \\ 0 & L_s & 0 \\ 0 & 0 & L_b \end{bmatrix}+\begin{bmatrix} E_{11} & E_{12} & 0 \\ E_{12} & 2E_{11} & 0 \\ 0 & 0 & E_{11} \end{bmatrix} \tag{24}$$

The elements of E_{11} and E_{12} in the above equation are defined as follows:

$$E_{11}=\sum_{m=1}^{n}\frac{-\Delta s\ \xi(s'_m)}{s_k-s'_m}$$

$$E_{12}=-\Delta s\ \xi(s'_m)\frac{a^2}{2c^2} \tag{25}$$

where n is the total number of discrete points separating integration panels, m and k are the source and field point index, respectively.

In addition, the elements of E_{11} has the zero value for the case where the source and field points are the same. Given this information, the correct formulation of a set of linear equations relating stokeslet and velocity for a chiral filament can be written as same Eq. (22).

The general transformation matrix to convert a vector described in local coordinates to the coordinate system fixed at the base of the helix taken from Eq. (9) is

$$\begin{Bmatrix} \hat{i} \\ \hat{j} \\ \hat{k} \end{Bmatrix} = \begin{bmatrix} h\frac{b}{c}\sin u' & -\frac{a}{c}\sin u' & -\cos u' \\ -\frac{b}{c}\cos u' & \left[h\frac{a}{c}\cos u'\right] & -h\sin u' \\ h\frac{a}{c} & \frac{b}{c} & 0 \end{bmatrix} \begin{Bmatrix} \hat{e}_n(s') \\ \hat{e}_s(s') \\ \hat{e}_b(s') \end{Bmatrix}$$
$$\equiv [A(u')]\,\hat{e}_\nu(s') \tag{26}$$

where $[A(u')]$ is called a unitary matrix, since the transpose of the matrix is equal to its inverse.

For instance, the correct way to formulate the problem is then to say

$$\begin{Bmatrix} V_{n4} \\ V_{s4} \\ V_{b4} \end{Bmatrix} = [M_{43}][A_4^{-1}][A_3] \begin{Bmatrix} \alpha_{n3} \\ \alpha_{s3} \\ \alpha_{b3} \end{Bmatrix} \tag{27}$$

In the above equation, the field point is #4, and we are determining the contribution to the velocity at that point from source point #3. Remember $[M_{43}]$ is directly from Johnson's integral equation, which is written in the field point coordinates.

The accuracy of the numerical schemes being used here were checked by Kim and Rae (1991). They compare the hydrodynamic resistance coefficients for a straight rigid ellipsoidal particle with the analytical formulas (Brenner 1964), and show excellent agreement.

4. Trajectories

From Newton's laws of motion, the total external force acting on the filament can be expressed by the sum of quasi-static hydrodynamic force, buoyant force and gravitational force. In addition, the total external torque at the center of mass consists of the torque due to the total hydrodynamic force and that due to the buoyant force. In the present study, the gravitational forces acting on the particle do not produce a torque because we assume the particles have a uniform density. Therefore, the translational and rotational motions of the center of mass can be written as dimensionless form:

$$F = Y\hat{s}_3 \tag{28}$$
$$T_c = 0 \tag{29}$$

where buoyancy parameter Y is proportional to the ratio of the terminal velocity due to gravitational settling, to the characteristic shear flow velocity, defined as:

$$Y \sim \frac{(m_p - m_f)\,g}{\mu G \ell^2} \tag{30}$$

Here m_p is the mass of the filament, m_f the mass of the fluid displaced by the filament.

From Eqs. (19), (20), (28) and (29), we have the following formulas for the linear and angular velocities of the chiral filament located in the four-roll flowfield:

$$\omega_c = B \cdot Y\hat{s}_3 + P : S \tag{31}$$
$$U_c - u_c = R \cdot Y\hat{s}_3 + Q : S \tag{32}$$

where the dyadics B, R, and triadics P, Q are defined as:

$$B = [K \cdot C_c^{-1} \cdot \Omega_c - C_c^{\dagger}]$$
$$R = -C_c^{-1} \cdot \Omega_c \cdot B$$
$$P = B \cdot (\Phi_c - K \cdot C_c^{-1} \cdot \Psi_c)$$
$$Q = [C_c^{\dagger} \cdot \Omega_c^{-1} \cdot C_c - K]^{-1} \cdot (\Phi_c - C_c^{\dagger} \cdot \Omega_c^{-1} \cdot \Psi_c)$$

If the filament is neutrally buoyant ($Y=0$), the linear and angular velocities are dependent only upon the third-rank tensors P and Q. From knowledge of these linear and angular velocities, the trajectories of a chiral filament can be found numerically.

The equations for the orientations of a chiral filament (see Fig. 1) are obtained by introducing the Euler angles ϕ, θ and δ (in this study we call them azimuthal, polar, and roll angles, respectively), and by the two sets of coordinates, one of which is filament-fixed, and the other space-fixed (further information see Goldstein 1980). With the help of Eq. (31), the time rate change of the orientation angles are calculated by using the following equations:

$$\frac{d}{dt}\begin{Bmatrix}\phi\\ \theta\\ \delta\end{Bmatrix} = -\frac{1}{\sin\theta}\begin{bmatrix}-\sin\delta & -\cos\delta & 0\\ -\sin\theta\cos\delta & \sin\theta\sin\delta & 0\\ \cos\theta\sin\delta & \cos\theta\cos\delta & -\sin\theta\end{bmatrix}\begin{Bmatrix}\omega_{c_1}\\ \omega_{c_2}\\ \omega_{c_3}\end{Bmatrix}$$
$$= -\frac{1}{\sin\theta}\begin{bmatrix}\sin\phi\cos\theta & -\cos\phi\cos\theta & -\sin\theta\\ -\cos\phi\sin\theta & -\sin\phi\sin\theta & 0\\ -\sin\phi & \cos\phi & 0\end{bmatrix}\begin{Bmatrix}\omega_{s_1}\\ \omega_{s_2}\\ \omega_{s_3}\end{Bmatrix} \quad (33)$$

Note that the roll angle history shows a jump due to the singularity at $\sin\theta=0$. This problem can be resolved by using cartesian rotations instead of Euler angles (Kim and Rae 1991). One way to avoid the singular behavior is to use the cartesian rotations whenever θ approached zero, switching back to the Euler angles when θ departs from zero. In the present work, we have used a simpler approach, namely, to set $d\phi/dt$ equal to zero whenever $|\sin\theta|$ is less than 0.015. This has the effect of putting all of the rotation into δ. The orientation of the particle is negligibly affected by this simplification.

In addition, the location of the center of mass in the space-fixed coordinates (s_1, s_2, s_3) is found from:

$$\frac{d\mathbf{s}}{dt} = U_c \quad (34)$$

where U_c is the translational velocity of the center of mass.

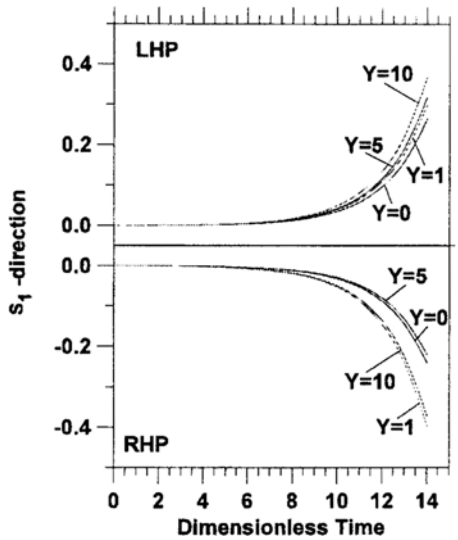

Fig. 3 Center of mass histories along the s_1-direction with an initial condition $\phi_i/\theta_i/\delta_i=0°/90°/90°$ in the rectangular hyperbolic flow

In order to find the variations of the angles and the center of mass location as a function of time, we have used a fourth-order Runge-Kutta scheme. The orientation of a chiral filament in a two-dimensional rectangular hyperbolic flow field evidently differs from that found when constant shear flow is involved, since the differences of nature of flow. The histories of left- and right-handed chiral filaments along the s_i-direction are shown in Figs. 3 to 5 for various values of

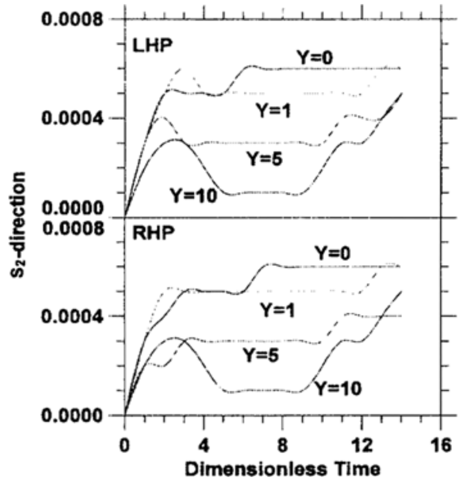

Fig. 4 Center of mass histories along the s_2-direction with an initial condition $\phi_i/\theta_i/\delta_i=0°/90°/90°$ in the rectangular hyperbolic flow

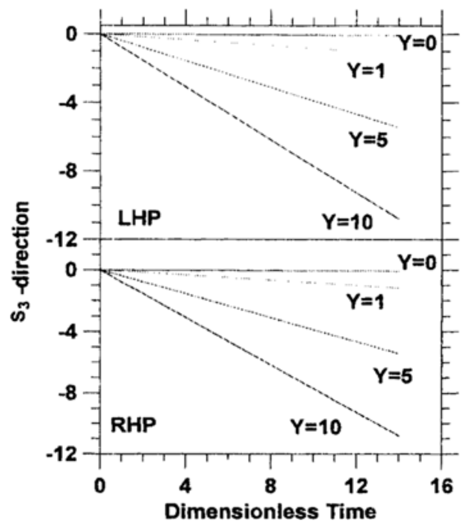

Fig. 5 Center of mass histories along the s_3-direction with an initial condition $\phi_i/\theta_i/\delta_i=0°/90°/90°$ in the rectangular hyperbolic flow

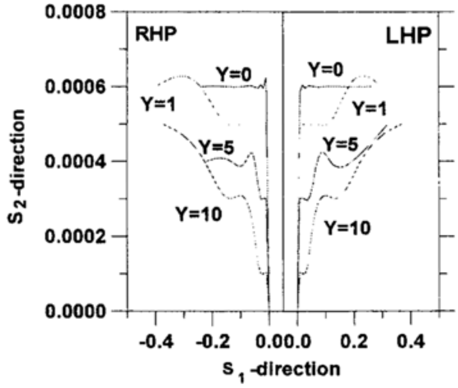

Fig. 6 Trajectories of chiral filaments with an initial condition $\phi_i/\theta_i/\delta_i = 0°/90°/90°$ in the s_1s_2-plane

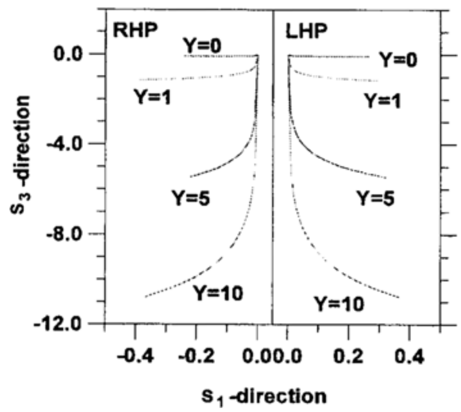

Fig. 7 Trajectories of chiral filaments with an initial condition $\phi_i/\theta_i/\delta_i = 0°/90°/90°$ in the s_1s_3-plane

buoyancy parameters. In figures LHP, RHP denote the left- and right-handed particle, respectively. Here the filament having the geometry $L/D=1$, $n=2$ and $d/2a=0.01$ is initially oriented by $\phi_i/\theta_i/\delta_i=0°/90°/90°$, and started from the origin. These figures show a separation between LHP and RHP along the s_1-migration, and a steady drift in the s_3-direction.

Figures 6 and 7 show the separating trajectories of the center of mass of the above filaments in the s_1s_2-and s_1s_3-plane for various values of Y. As the relative importance of gravity increases, a point is reached where the particle rotation due to sedimentation becomes comparable to that induced by the four-roll flow. At this point, it is possible for a filament of chirality to settle without rotation. We may have deduced that the sedimentation velocity is affected by buoyancy parameter.

5. Conclusions

We have presented solution for the creeping flow over a chiral filament in the two-dimensional rectangular hyperbolic flow field with the various buoyancy parameters. More specifically, using Johnson's slender body theory, we were able to find the force and torque required to move a chiral filament in any direction. These results were then expressed in the context of the hydrodynamic resistance coefficients, such as, second- and third-rank tensors, so that all motions can be described at once for a given orientation.

For better understanding of motion for filaments of neutral buoyancy, however, it may be necessary to include the effects of apparent mass and the viscous history forces described by the Bassett integral in the equations of the particle motion. This will be presented in the future, including the phase-plane analysis to predict terminal translational velocities.

The main objectives of this paper are to make some developments that enable the results of these theories to be tested experimentally. The flows studied here are typical of those occurring in practice, and these results can be used to predict the behavior of suspensions in such flows.

References

Boikess, R. S. and Edelson, E., 1981, *Chemical Principles,* Harper & Row, New York.

Brenner, H., 1964, "The Stokes Resistance of an Arbitrary Particle-III. Shear Field," *Chemical Eng. Sci.*, Vol. 19, pp. 631~651.

Chaffey, C. E., Takano, M., and Mason, S. C., 1965, "Particle Motions in Sheared suspensions, XVI. Orientation of Rods and Disks in Hyperbolic and Other Flows," *Cand. J. Phys.*, Vol. 43, pp. 1269~1287.

Goldsmith, H. L., 1971, "Red Cell Motions and

Wall Interactions in Tube Flow," *Federation Proceedings*, Vol. 30, pp. 1578～1590.

Goldsmith, H. L. and Mason, S. G., 1971, "Particle Motions in Sheared Suspensions, XIII. The Spin and Rotation of Disks," *J. Fluid Mech.*, Vol. 12, pp. 88～96.

Goldstein, H., 1980, *Classical Mechanics*, 2nd ed., Addison-Wesley Publ. Co. Inc., Cambridge, Massachusetts.

Happel, J. and Brenner, H., 1986, *Low Reynolds Number Hydrodynamics*, Martinus Nijhoff Publishers, Boston.

Jeffery, G. B., 1922, "The Motion of Ellipsoidal Particles Immersed in a Viscous Fluid," *Proc. R. Soc. London A*, Vol. 102, pp. 161～179.

Johnson, R. E., 1977, "Slender-Body Theory for Stokes Flow and Flagellar Hydrodynamics," Ph. D. thesis, California Institute of Technology.

Johnson, R. E., 1980, "An Improved Slender-Body Theory for Stokes Flow," *J. Fluid Mech.*, Vol. 99, pp. 411～431.

Kim, S. and Karrila, S. J., 1991, *Microhydrodynamics*, Butterworth-Heinemann, Boston.

Kim, Y. J. and Rae, W. J., 1991, "Separation of Screw-Sensed Particles in a Homogeneous Shear field," *Int. J. Multiphase Flow*, Vol. 17, No. 6, pp. 717～744.

Leal, L. G., 1984, "Birefringence Studies of Flow-Induced Conformation Changes in Polymer Solutions," *Proc. IX Intl. Congress on Rheology*, Mexico, pp. 191～209.

Press, W. H., Flannery, B. P., Teukolsky, S. A. and Vetterling, W. T., 1986, *Numerical Recipes*, Cambridge University Press.

Stover, C. A. and Cohen, C., 1990, "The Motion of Rodlike Particles in the Pressure-Driven Flow Between Two Flat Plates," *Rheologica Acta*, Vol. 29, pp. 192～203.

Struik, D. J., 1950, *Differential Geometry*, Addition-Wesley Press, Cambridge, Massachusetts.